Observations of cavitation erosion pit formation

Matevž Dular, Olivier Coutier Delgosha, Martin Petkovšek

PII: S1350-4177(13)00038-2
DOI: http://dx.doi.org/10.1016/j.ultsonch.2013.01.011
Reference: ULTSON 2256

To appear in: *Ultrasonics Sonochemistry*

Received Date: 2 April 2012
Revised Date: 17 January 2013
Accepted Date: 19 January 2013

Please cite this article as: M. Dular, O.C. Delgosha, M. Petkovšek, Observations of cavitation erosion pit formation, *Ultrasonics Sonochemistry* (2013), doi: http://dx.doi.org/10.1016/j.ultsonch.2013.01.011

Observations of cavitation erosion pit formation

Matevž Dular (corresponding author)
Laboratory for Water and Turbine Machines, University of Ljubljana
Askerceva 6, 1000 Ljubljana, Slovenia
matevz.dular@fs.uni-lj.si
Tel: +386 1 4771 453
Fax: +386 1 2518 567

Olivier Coutier Delgosha
Laboratoire de Mécanique de Lille, ParisTech
8 Boulevard Louis XIV, 59046 Lille, France
olivier.coutier@ensam.eu

Martin Petkovšek
Laboratory for Water and Turbine Machines, University of Ljubljana
Askerceva 6, 1000 Ljubljana, Slovenia
martin.petkovsek@fs.uni-lj.si

Abstract
Previous investigations showed that a single cavitation bubble collapse can cause more than one erosion pit (Philipp & Lauterborn [1]). But our preliminary study showed just the opposite – that in some cases a single cavitation pit can result from more than one cavitation event. The present study shows deeper investigation of this phenomenon. An investigation of the erosion effects of ultrasonic cavitation on a thin aluminum foil was made. In the study we observed the formation of individual pits by means of high speed cameras (>1000 fps) and quantitatively evaluated the series of images by stereoscopy and the shape from shading method. This enabled the reconstruction of the time evolution of the pit shape. Results show how the foil is deformed several times before a hole is finally punctured. It was determined that larger single pits result from several impacts of shock waves on the same area, which means that they are merely special cases of pit clusters (pit clusters where pits overlap perfectly). Finally it was shown that a thin foil, which is subjected to cavitation, behaves as a membrane. It was concluded that the physics behind erosion depends significantly on the means of generating cavitation (acoustic, hydrodynamic, laser light) and the specimen characteristics (thin foil, massive specimen), which makes comparison of results of materials resistance to cavitation from different experimental set-ups questionable.
Further development of the shape from shading method in the scope of cavitation erosion testing will enable better evaluation of cavitation erosion models.

1 Introduction

Cavitation describes the formation and the consequent collapse of bubbles in a liquid. It occurs when a liquid is subjected to rapid changes of pressure. In most cases it is undesired as it is accompanied by effects like noise, vibration, drop in efficiency of turbine machines and also by erosion of the solid surfaces of the flow tract.

We can distinguish two main periods in the cavitation erosion process. The incubation period where only small plastic deformations (pits) can be seen, which is followed by the second period during

which the material separates from the surface, first at an exponential and later at a linear rate (Franc & Michel [2]).
The damage within incubation period is usually evaluated visually according to the number, and the size of the pits (Dular et al. [3]), later on, during the mass loss period the damage can only be evaluated by weighting or by profilomerty (Bachert et al. [4]).
Many authors (Zeqiri et al. [5], Laborde et al. [6], Krefting et al. [7], Dular & Osterman [8]) used thin metal foil for to estimate the erosion, but these studies all lack in detailed and qualitative evaluation of the damage.

Previous investigations showed that a single cavitation bubble collapse can cause more than one erosion pit (Philipp & Lauterborn [1]). But our preliminary study showed just the opposite – that in some cases a single cavitation pit can result from more than one cavitation cloud collapse. We observed the aluminum foil from both sides at a frame rate of 4000 fps. Cavitation structures formed only on the front side, hence we could observe pit formation from the back side of the foil. Figure 1 shows a sequence of bubble cloud growth, collapse and two rebounds – three collapses of cavitation cloud occur at the same position shortly one after another.

Figure 2 shows the deformation of the foil that was recorded simultaneously with the images in Fig. 1. The quality of the images was too poor for advanced evaluation; hence the data can only be used for qualitative explanation of the phenomenon.

One can see that the pit grows when the cavitation cloud on the other side of the foil is most active (shortly before it collapses to its minimum volume). This occurs three times in the present case, hence showing that more than one collapse can be involved in a single pit formation.

The present study shows deeper investigation of this new phenomenon. Cavitation was generated by means of ultrasound in a small cylindrical vessel. A thin aluminum foil was used as a sensor for cavitation erosion. We used two high resolution high speed cameras to observe pit formation.
To evaluate the damage caused by cavitation we used stereoscopic imaging and the shape from shading method. This way the damage could be quantitatively evaluated at a very high frequency (1000Hz or more in the present case). This is a breakthrough compared to the methods employed previously, which allowed only very limited insight into the evolution of the damage as detailed evaluation could only be performed when the cavitation process was stopped (every several minutes for example – Osterman et al. [9]).

2 Experiment

2.1 Set-up

Figure 3 shows the experimental set-up. On the left picture the set-up (without holders for the cylinder) and on the right one the position of the cameras are presented.

A small, 140 mm high and 72 mm in diameter, cylindrical vessel made out of stainless steel, was used for the experiments. A 50 W, 40 kHz piezo actuator was used to generate cavitation. The ultrasound frequency was carried by low frequency of electrical network (50 Hz), hence cavitation was only triggered for a short period of time every $1/50^{th}$ of a second.

The cameras were positioned at a distance of 500 mm from the surface of the aluminum foil. The angles α, β and γ were set in a way that enabled surface shape reconstruction. The values were: α =

65°, β = 65° and γ = 65°.

MotionBLITZ EoSens mini1 high speed CCD cameras were used to capture the images of the foils surface. The region of interest varied – the resolution was 30 μm/pixel. A continuous light source VEGA VELUM150DR (lamp: EKE 21V 150W) was used for illumination.

A 10 μm thick aluminum foil was used as erosion "detector". It was mounted on a cylinder with an inner diameter of 40 mm and submerged into the vessel. The water level inside the cylinder was the same as the level in the vessel. The foil was positioned in the centre of the vessel 112 mm (3 wave lengths) from the bottom. The level of water was always 10 mm above the position of the foil.

Unprepared water was used for the experiments which were performed under constant atmospheric pressure of 985 mbar and at a constant temperature of 25 °C.

2.2 Evaluation

Different methods for reconstruction of objects shape from its image or images exist. In addition to binocular disparity, shading, texture, and focus all play a role in how we perceive shape. The study of how shape can be inferred from such cues is called shape from "x", since the individual instances are called shape from shading, shape from texture, and shape from focus (Szeliski [10]). Each method comes with its own limitations, advantages and costs.

In the present study the shape in question is constantly changing but the texture remains unchanged. Improving the shape from shading algorithm by application of light from different directions (photometric stereo) is not possible due to the unsteady nature of the case. Finally shape from shading algorithm was used to reconstruct the shape from each of the two images taken from different perspectives which is a method similar to the photometric stereo addition by Zhang et al. [11].

2.2.1 The algorithm

We assume that the surface under consideration is of a uniform albedo and reflectance, and that the light source directions and camera positions are known. Under the assumptions of distant light sources and observer, the variation in intensity becomes purely a function of the local surface orientation.

$$I(x,y) = R(p(x,y),q(x,y)), \tag{1}$$

where $(p, q) = (z_x , z_y)$ are the depth map derivatives and $R(p, q)$ is called the reflectance map, which is defined as the non-negative dot product between the surface normal $\hat{\mathbf{n}} = (p,q,1)/\sqrt{1+p^2+q^2}$ and the light source direction $\mathbf{v} = (v_x, v_y, v_z)$:

$$R(p,q) = max\left(0, \rho \frac{pv_x + qv_y + v_z}{\sqrt{1+p^2+q^2}}\right), \tag{2}$$

where ρ is the surface reflectance factor (albedo). Eqns. 1 and 2 can be used to estimate *(p,q)* using non-linear least squares method. But additional constraints have to be imposed, since there are more unknowns per pixel *(p,q)* than there are measurements *(I)*. Instead of first recovering the orientation fields *(p,q)* and integrating them to obtain a surface, we can directly minimize the discrepancy in the image formation (Eqn. 1) while finding the optimal depth map *z(x,y)* (Horn [12]).

To improve the algorithm we combined the shape from shading technique with photometric stereo. For each camera position we have a different reflectance map, $R_1(p,q)$ and $R_2(p,q)$. Each pixel then has two intensities I_1 and I_2. With this data we can recover both an unknown albedo ρ and a surface orientation estimate *(p,q)*. We get a set of linear equations of the form:

$$I_k = \rho\, \hat{\mathbf{n}} \cdot v_k \,, \qquad (3)$$

from which we can recover $\rho\hat{\mathbf{n}}$ using linear least squares. Once the surface normals or gradients have been recovered at each pixel, they can be integrated into a depth map using a variant of regularized surface fitting (Harker & O'Leary [13]).

2.2.2 Test case

To evaluate the algorithm we took a surface with a known geometry and captured several pictures of it. The test object is a half sphere with a diameter of 40 mm. The color and albedo of the surface resembled the one of the aluminum foil. Figure 4 shows an image of the surface (left) and the surface diagram of the reconstructed shape (middle) and the real and calculated cross-sections through the middle of the object (right).

From the comparison we see that there are some discrepancies between the real and calculated shape. Analysis showed that the shape can be determined within about 10 to 15% of the real one. This value is larger of the one of laser profiler but comparable to the simpler methods like pit-count (Dular et al. [3]), and therefore sufficient for the present study.

3 Results and Discussion

Figure 5 shows 4 foils after about 10 seconds of exposure to cavitation.

One can see that the final extent of the damage varies significantly between the cases. Also the topology of deformation is different. In one case single pits form, while in other pits tend to cluster. The reason for this lies in a stochastic nature of cavitation and also its tendency to develop in regions with more imperfections (Dular & Osterman [8]) – although great care was given to the application of the aluminum foil, some imperfections could remain present. Since the purpose of the study was to investigate how the foil is deformed and not what damage was caused by cavitation, such discrepancies played no role in the quality of the study – one could even treat it as beneficial since more situations could be observed without changing the set-up of the experiment.

The purpose of the study was to investigate the formation of a single pit or a pit cluster. Hence one or more regions of interest could be selected on a foil for each experiment. The sequence in Fig. 6 shows

the formation of a single pit. In this particular case the images were captured at a frame rate of 1842 fps, but only images taken approximately every 20 ms are shown (20 ms corresponds to 50 Hz of the ultrasound carrying frequency – images show situation just after the end of each deformation phase). The image is geometrically transformed so that the shape of the pit is shown as if the camera is positioned directly above it and that the light source comes from the side.

It is evident that the foil is deformed several times during the experiment. This implies that it sustains damage from a series of cavitation bubble (or cloud) collapses. We believe that this phenomenon is only present in the case of acoustic, electrical discharge and laser light cavitation where bubbles can grow and collapse at the same position – in the case of hydrodynamic cavitation the position of cloud implosion, where the damage is the greatest, is far away from the position of cavitation growth as the clouds are convected downstream by the flow. Firstly two pits form that later merge. Finally the pit grows and reaches a diameter of about 1.5 mm after 0.124 seconds of exposure to cavitation. As expected the experiment confirmed that the foil deforms approximately every 20 ms what corresponds to the frequency that carries ultrasonic oscillations (50 Hz). The time of deformation during each cycle is in average 1.8 ms long, but can vary significantly (times as low as 0.6 ms and as high as 4 ms were seen, although such extremes were rare).

To look into the process in even more detail a sequence showing just one deformation of the foil is shown in Fig. 7. The images correspond to the first deformation of the foil in Fig. 6.

The deformation of the pit in Fig. 7 occurred during a single cavitation event. The time delay between images is 0.54 ms. As already mentioned it takes in average 1.8 ms for the foil to deform. In this particular case the diameter of the pit grew to about 0.7 mm in this period.

It was also common to observe the formation of pit clusters (partially overlapping pits). A typical situation is shown in Fig. 8. The images were captured at a frame rate of 1723 fps, but only every 60^{th} image is shown (time delay is about 35 ms).

In essence this is the same but more general process as a single pit formation. Deformation takes place in the same region but not at an exactly the same position. Hence more than one pit forms. It is interesting that the pit clusters tend to grow much faster than single pits. This is again related to the self amplification phenomenon – pit clusters have a more arbitrary and irregular shape than single pits, and are therefore better nucleation sites. Additional reason for the faster growth of pit clusters is probably the decreased resistance of the material in that region.

Rupturing of the foil was rarely observed within the maximal time of recording (about 10 seconds). Sequence in Fig. 9 shows such a case, where foil was first deformed and then punctured. Eventually a larger hole formed. Time delay between the images is 0.3 s – the sequence is about 6 s long.

Pits start to accumulate in a line – the reason probably lies in the fact that cavitation forms in a shape of a streamer (Mettin [14]) which consists linear streaks of bubbles that travel rapidly from one end to the other, forming a directed bubble stream. After about 1.5 s (picture 5) the foil is ruptured on the right side of the image. The imperfection than acts as a “cavitation generator” that triggers more cavitation activity and more mass is lost in this region. In the final stage a large (about 5 by 1 mm big) hole is eroded (it is the largest in the place where the foil was first ruptured).

Reconstruction of the shape of pits and pit clusters is of a great importance for determining the physics behind cavitation erosion and for the development of cavitation erosion models. Previously it was possible to perform such an analysis only in longer intervals (minutes). We used Shape Form Shading algorithm to reconstruct the shape of pits and pit clusters. Diagrams in Figs. 10 and 11 are inverted for better and easier presentation – highest point corresponds to the greatest depth of the pit. Fig. 10 shows the evolution of the shape of a single pit that formed after several cloud collapses. The time difference between the images is 14 ms.

It can be seen that foil sustained several impacts during the experiment. First two smaller pits formed in vicinity of each other (pictures 3, 4 and 5). After that additional impacts caused merging of the pits into a bigger one (picture 6), but some evidence that it was initiated from two single pits remains (two small peaks at the highest point). At the end of the experiment the pit grew to a depth of about 40 μm and diameter 1.5 mm. This values are much larger than the ones we usually observe in cavitation erosion of a solid material (for example 5 μm depth and 0.25 mm diameter according to Franc [15]) what can be contributed to the very thin nature of foil that behaves more like a membrane which is also stretched when stress is applied.

Also the formation of a pit cluster was reconstructed, what is shown in Fig. 11. The time difference between the images is 50 ms.

Previous figure (Fig. 10) shows a formation of a single pit which results from several cloud collapses – it can be claimed that a single pit forms purely by chance and is not likely to occur. More general type of deformation is the pit cluster (Fig. 11). Here single pits resulting from individual cloud collapses only partially overlap, hence a much more heterogeneous surface forms. Nevertheless a deformation of the foil at a specific position influences the already existent pits in the vicinity that can either grow further or (less likely) flatten out due to the membrane nature of the thin aluminum foil. The distribution of the pits on a small scale is arbitrary – it may appear that they tend to cluster in lower corner (high x and low y value) but the size of the region of interest is approximately the same as the size of cavitation structures so the influence of position can be ruled out. The maximum pit depth at the end of the experiment was about 0.1 mm.

Interesting is also the evolution of the pit and pit cluster volume in time, what is shown in Fig. 12.

It is evident that damaging of the surface occurs during a very short period that lasts a few ms during which the bubble cloud is excited by ultrasound. Damaging is periodic with a time interval of 20 ms what corresponds to the ultrasound carrying frequency of 50 Hz. In both cases (single pit and pit cluster) the rate of damaging decreases with time. Resemblance is expected since, as we discussed before, a single pit is only a special case of a pit cluster where pits are overlapping. The decrease of the damage rate is probably a result of stretching of the aluminum foil – it becomes more and more rigid until eventually a hole is punctured. The process is similar to the work hardening of ductile material when exposed to cavitation (Franc [15]).

4 Conclusions

Study shows high speed image acquisition of images of deformation on a foil due to cavitation. Results, of this first time study, show how a pit and a pit cluster are formed. Single deformation of the foil takes approximately the same amount of time as the time of cavitation cloud collapse. In contrast to previous studies (Philipp & Lauterborn [1]) which show that a single cavitation event can cause

multiple pits the present study showed just the opposite – that in some cases a single cavitation pit can result from more than one cavitation cloud collapse – a formation of a larger single pit during a longer experiment can actually be a cluster of pits that overlap perfectly solely by chance.
Clustering of pits in ultrasonic cavitation was also observed on much harder materials like fused silica glass, soda lime glass and amorphous metals [16, 17]. The effects described in the present study can therefore be attributed solely to the cavitation and not to the possible vibrating motion suffered by the soft material (thin foil) used in the present study.
A novel evaluation technique was used – shape from shading algorithm proved to be a useful tool for high speed cavitation damage measurements as long as we are dealing only with incubation period and when the image resolution is sufficient. The method has an obvious advantage that one can evaluate the erosion process at a very high frequency Methods employed previously allowed only very limited insight into the evolution of the damage as evaluation could only be performed when the cavitation process was stopped (every several minutes for example – Osterman et al. [9]). Further development of the method will enable acquisition of data that will be used for evaluation of cavitation erosion models – these usually base on physics of short time scales (single or several cavitation events) but have to rely on experimental data from longer experiments (minutes or even hours of exposure to cavitating flow) – Dular & Coutier [18].
As in the paper by Dular & Osterman [3] pit clustering due to self amplification process was observed. We believe that this phenomenon is only present in the case of cavitation generated by ultrasound, electrical discharge and laser light where bubbles grow and collapse at the same position. In the case of hydrodynamic cavitation bubbles appear at the position of the lowest pressure (at the leading edge of the blade for example). Then they are convected downstream by the flow and implode in a higher pressure region – far away and independently of the position of their origin. This difference in physical background explains why sometimes a material that was found to be “cavitation resistant” real applications fails when it is tested by the standard ASTM G32 – 10 test [19] or vice versa (Chahine [20]).
Finally it was also found that a thin foil behaves like a membrane which is stretched when stress is applied. We found that the pits were much larger than in the reported cases where solid material was used as a specimen (Franc [15]). This again raises a question whether results of studies where erosion is generated by acoustic and hydrodynamic cavitation and solid and thin foil specimens can be compared.

References

[1] A. Philipp, W. Lauterborn, Cavitation erosion by single laser-produced bubbles, J. Fluid Mech. 361 (1998), 75–116.

[2] J.P. Franc, J.M. Michel, Fundamentals of Cavitation, Kluwer Academic Publishers, 2004.

[3] M. Dular, B. Bachert, B. Stoffel, B. Sirok, Relationship between cavitation structures and cavitation damage, Wear 257 (2004) 1176-1184.

[4] B. Bachert, G. Ludwig, B. Stoffel, S. Baumgarten, Comparison of different methods for the evaluation of cavitation damaged surfaces, in: ASME Fluids Engineering Division Summer Meeting and Exhibition, Houston, 2005.

[5] B. Zeqiri, M. Hodnett, A.J. Carroll, Studies of a novel sensor for assessing the spatial distribution of cavitation activity within ultrasonic cleaning vessels, Ultrasonics 44 (2006) 73-82.

- - , Acoustic cavitation field prediction at low and high frequency ultrasounds, Ultrasonics 36 (1998) 581-587.

[7] D. Krefting, R. Mettin, W. Lauterborn, High-speed observation of acoustic cavitation erosion in multibubble systems, Ultrasonics Sonochemistry 11 (2004) 119-123.

[8] M. Dular, A. Osterman, Pit clustering in cavitation erosion, Wear 265 (2008) 811-820.

[9] A. Osterman, B. Bachert, B. Širok, M. Dular, Time dependant measurements of cavitation damage , Wear 266 (2009) 945–951.

[10] R. Szeliski Computer Vision: Algorithms and Applications, 1st Edition, Springer-Verlag London Limited, 2011.

[11] R. Zhang, P.S. Tsai, J.E. Cryer, M. Shah, Shape from shading: A survey, IEEE Transactions on Pattern Analysis and Machine Intelligence 21/8 (1999) 690–706.

[12] B.K.P. Horn, Obtaining shape from shading information, Shape from Shading, MIT press, 1989.

[13] M. Harker, P. O'Leary, Least squares surface reconstruction from measured gradient fields, In IEEE Computer Society Conference on Computer Vision and Pattern Recognition Anchorage, 2008.

[14] R. Mettin, Bubble structures in acoustic cavitation, Bubble and Particle Dynamics in Acoustic Fields: Modern Trends and Applications, Research Signpost, Kerala, 2005.

[15] J.P. Franc, Incubation Time and Cavitation Erosion Rate of Work-Hardening Materials, Journal of Fluids Engineering 131/2, (2009), 021313.

[16] M. Virot, T. Chave, S. I. Nikitenko, D. G. Shchukin, T. Zemb, H. Moehwald, Acoustic Cavitation at the Water-Glass Interface, J. Phys. Chem. C 114 (2010) 13083–13091.

[17] D. Drozdz, R. K. Wunderlich, H.-J. Fecht, Cavitation Erosion Behaviour of Zr-Based Bulk Metallic Glasses. Wear 262 (2007) 176–183.

[18] M. Dular, O. Coutier-Delgosha Numerical modelling of cavitation erosion, Int. Journal of Numerical Methods in Fluids 61. (2009), 1388–1410.

[19] ASTM G32 - 10 Standard Test Method for Cavitation Erosion Using Vibratory Apparatus, ASTM International, 100 Barr Harbour Dr. PO Box C-700 West Conshohocken, Pennsylvania 19428-2959, United States

[20] G. L. Chahine, Development of cavitation erosion prediction method and procedures, International workshop on advanced experimental and numerical techniques for cavitation erosion prediction, Grenoble, March 1st and 2nd, 2011.

Figure captions

Fig. 1: Growth and collapse and two rebounds of a bubble cloud

Fig. 2: Formation of a single cavitation pit

Fig. 3: Experimental set-up.

Fig. 4: Test of the algorithm: image of the object (left), real and calculated object shape (middle and right)

Fig. 5: Foils after about 10 second of exposure to cavitation.

Fig. 6: Formation of a single pit.

Fig. 7: Single deformation of the foil.

Fig. 8: Formation of a pit cluster.

Fig. 9: From deformation to mass loss.

Fig. 10: Reconstructed shape of a single pit at different times.

Fig. 11: Reconstructed shape of a pit cluster at different times.

Fig. 12: Volume of a single pit (left) and pit cluster (right) as function of time.

Figure01

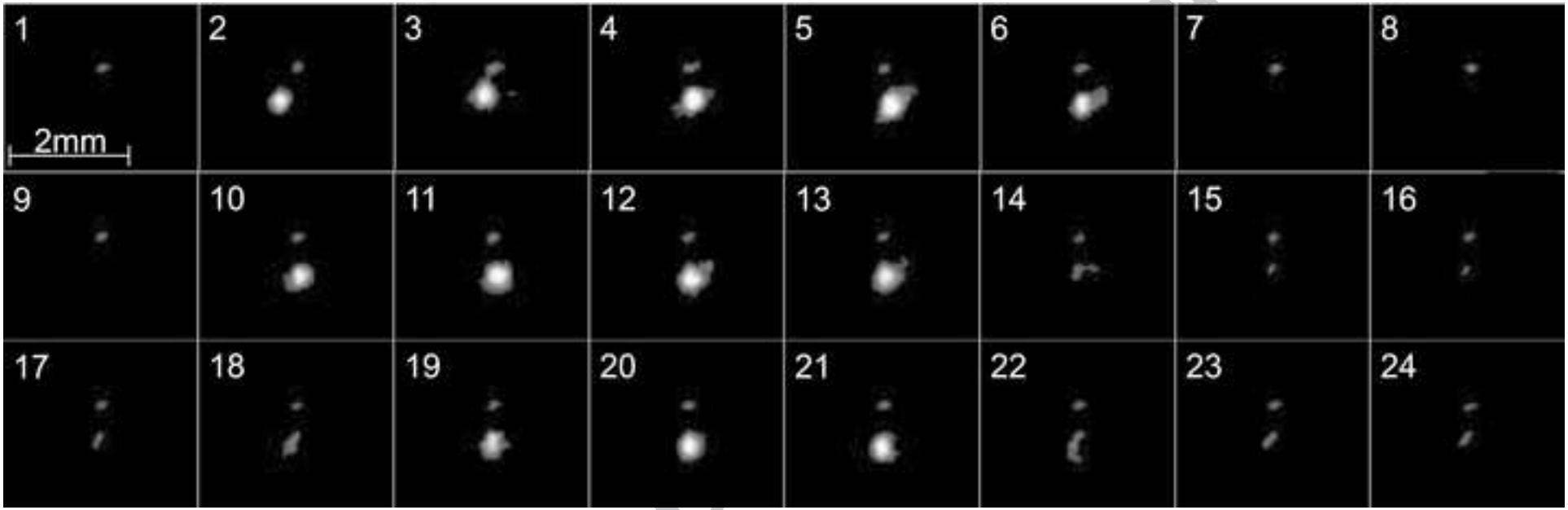

Figure02

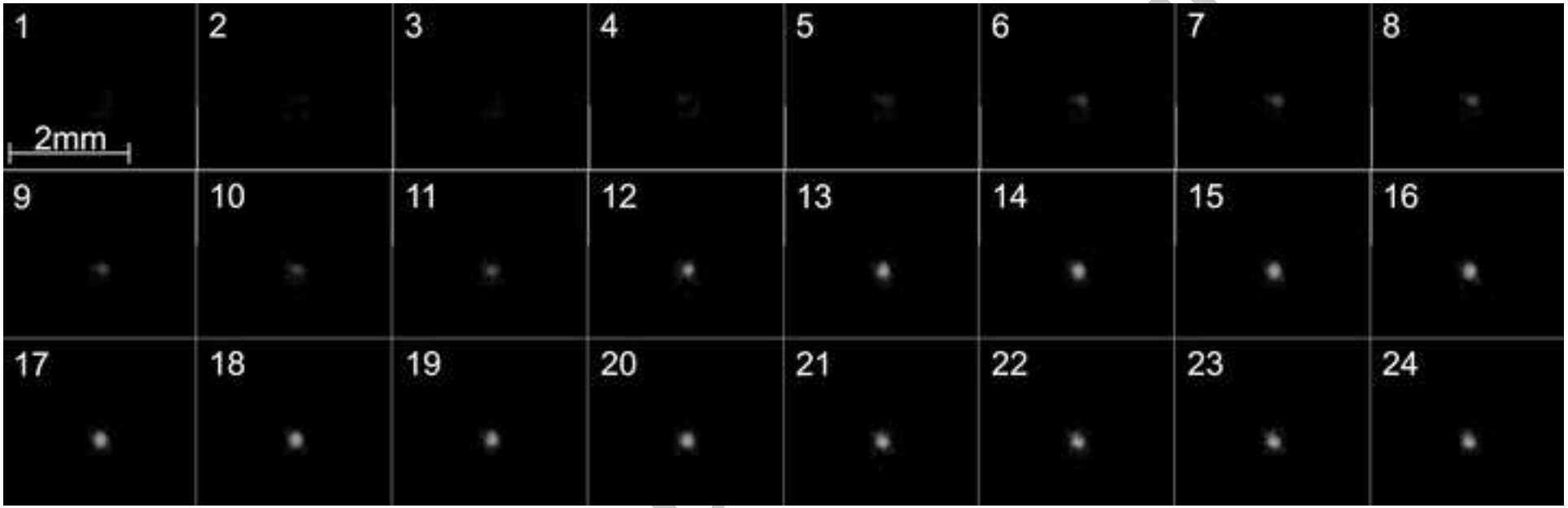

Figure03

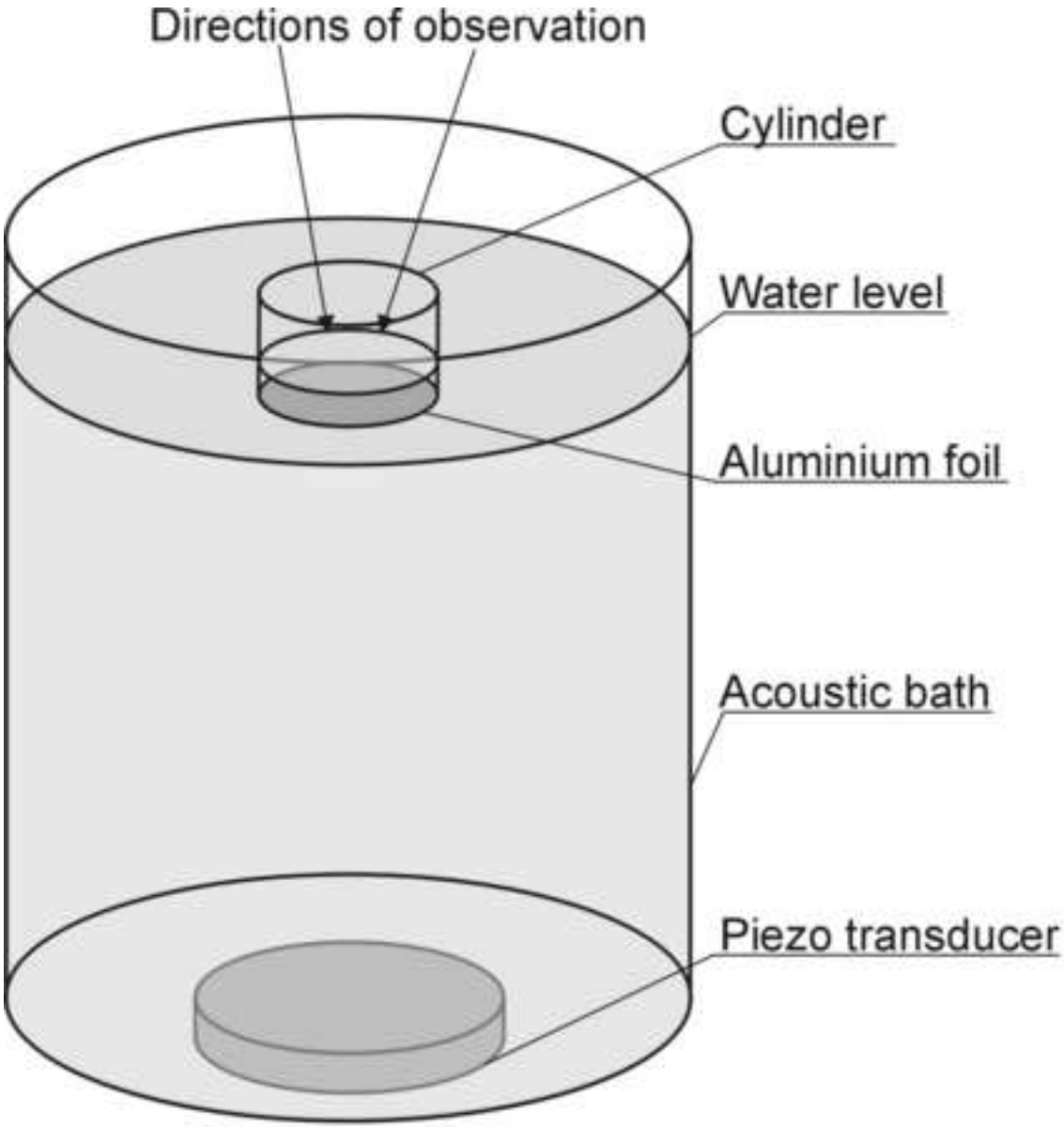

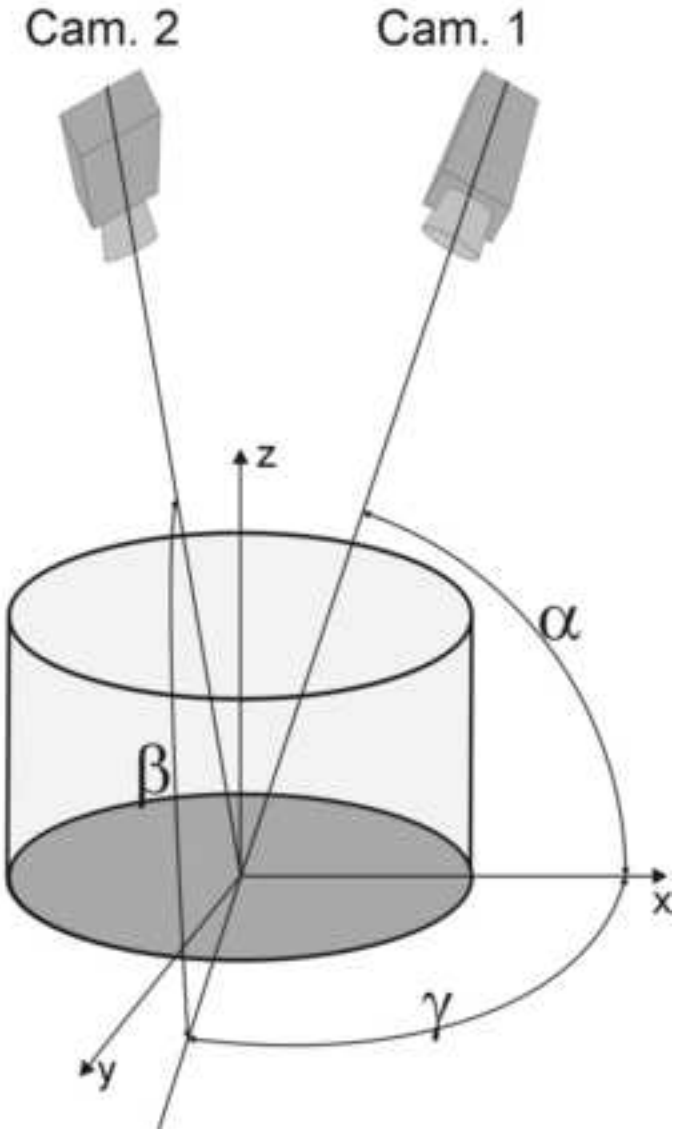

Figure04

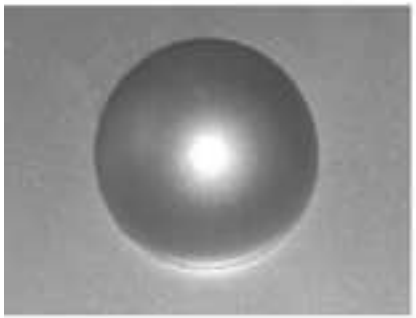

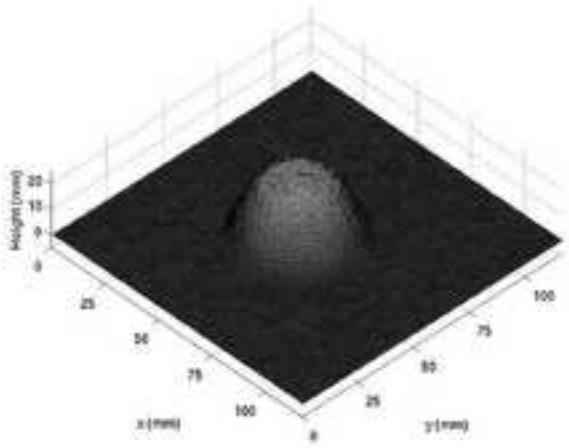

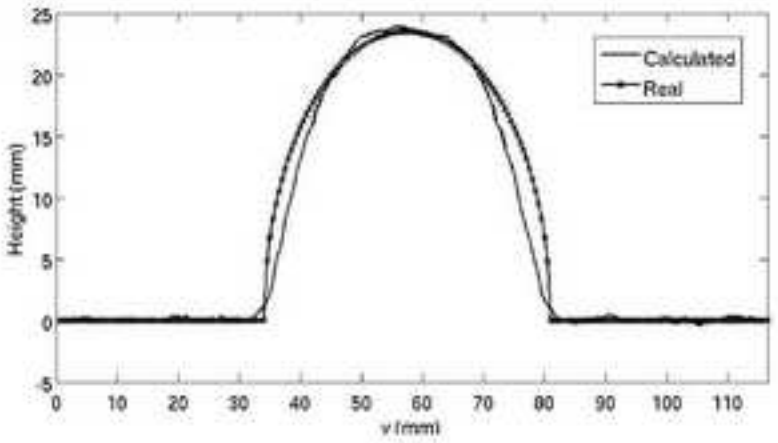

Figure05

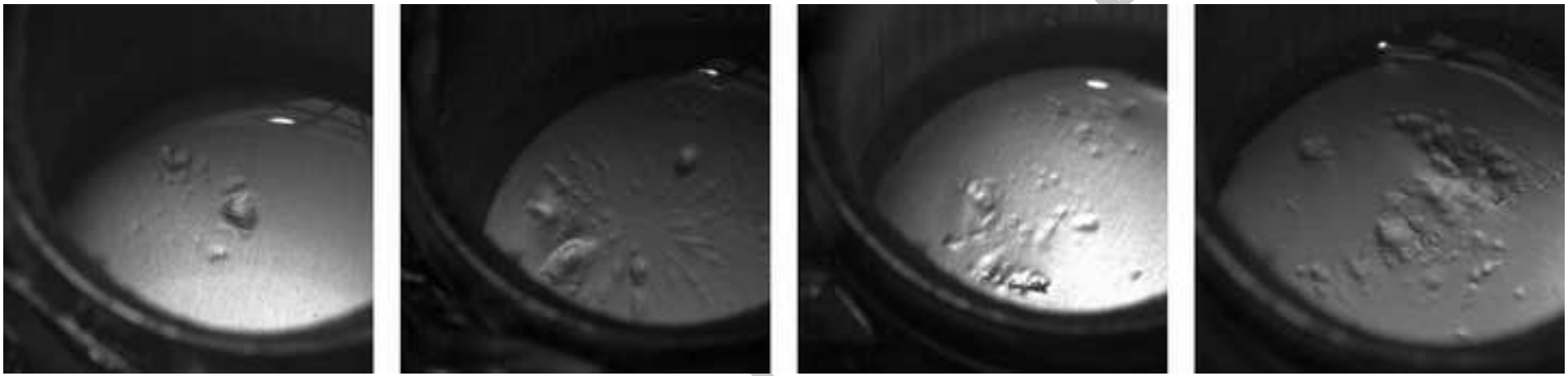

Figure06

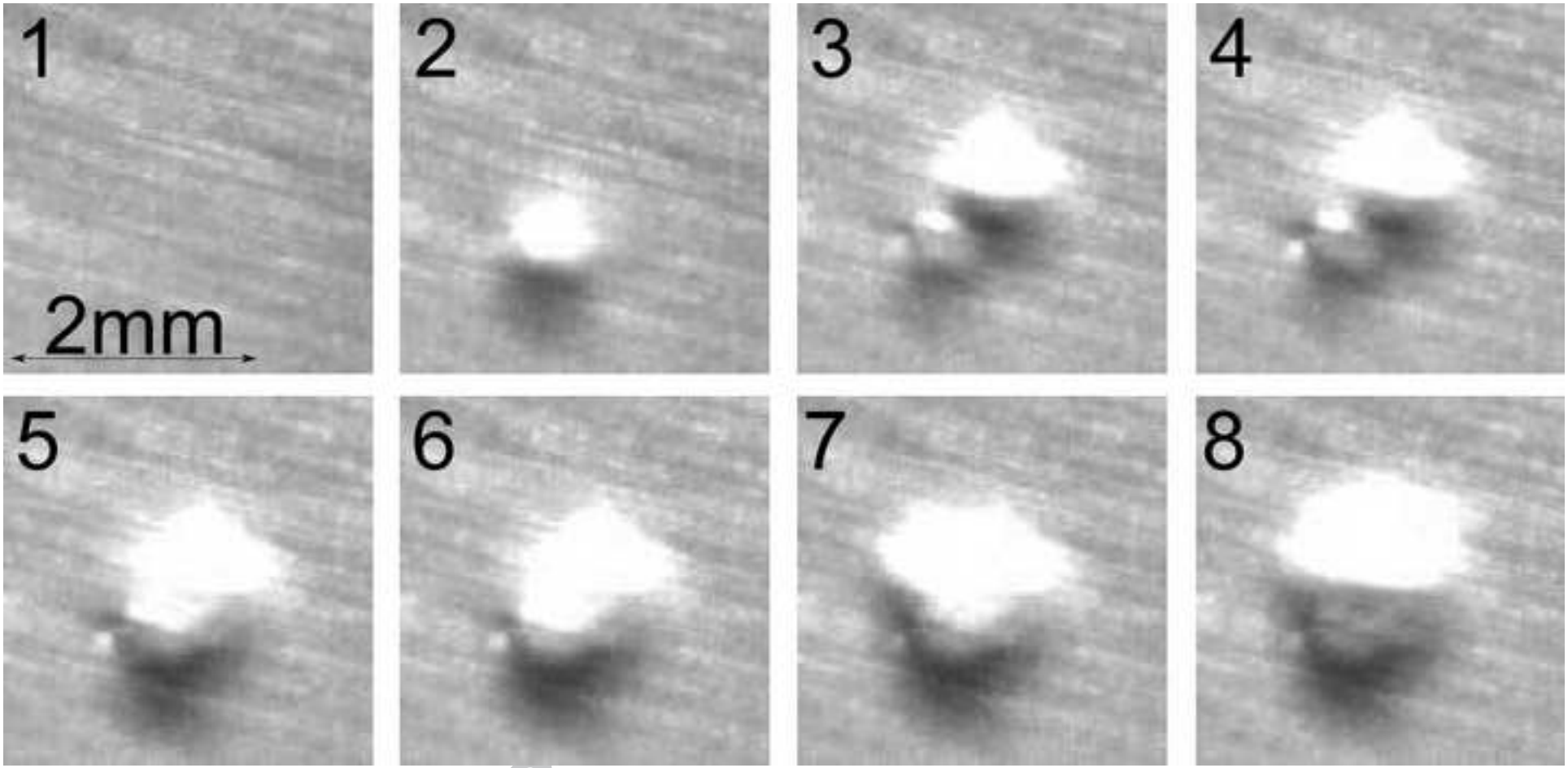

Figure07

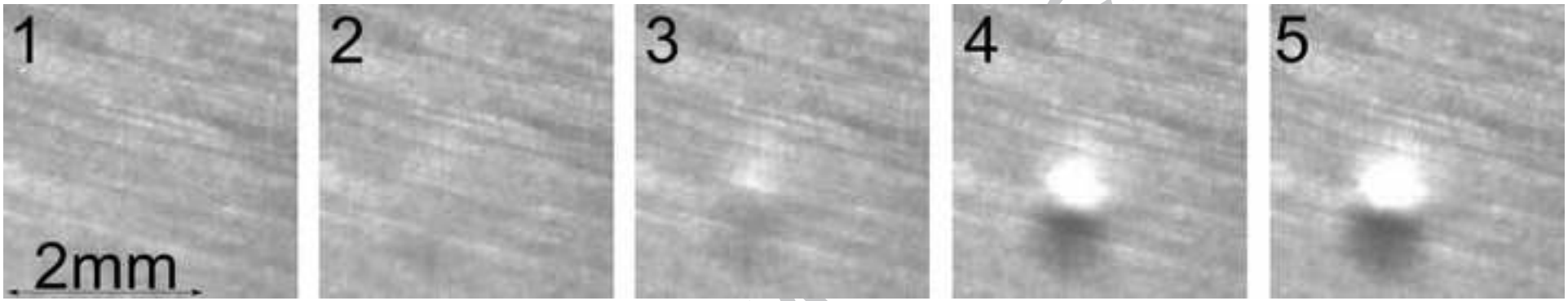

Figure08

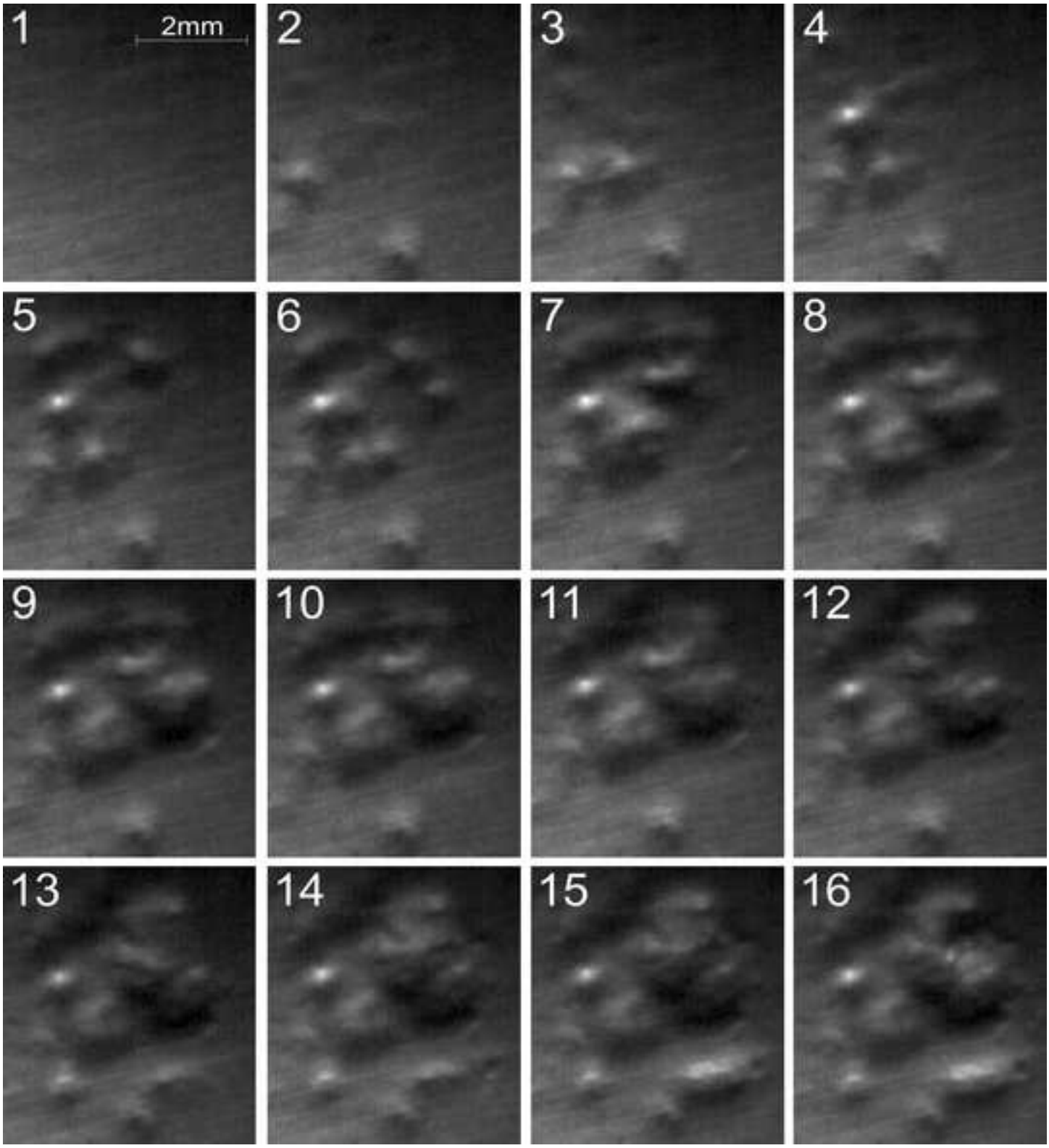

Figure09

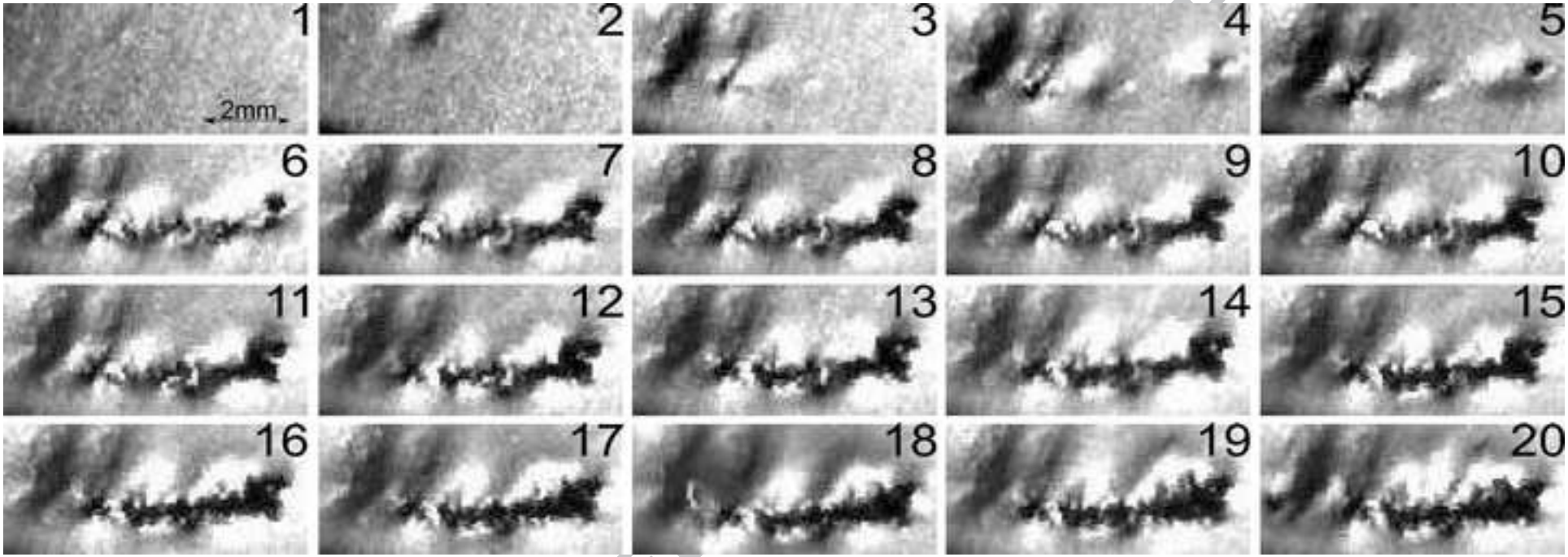

Figure10

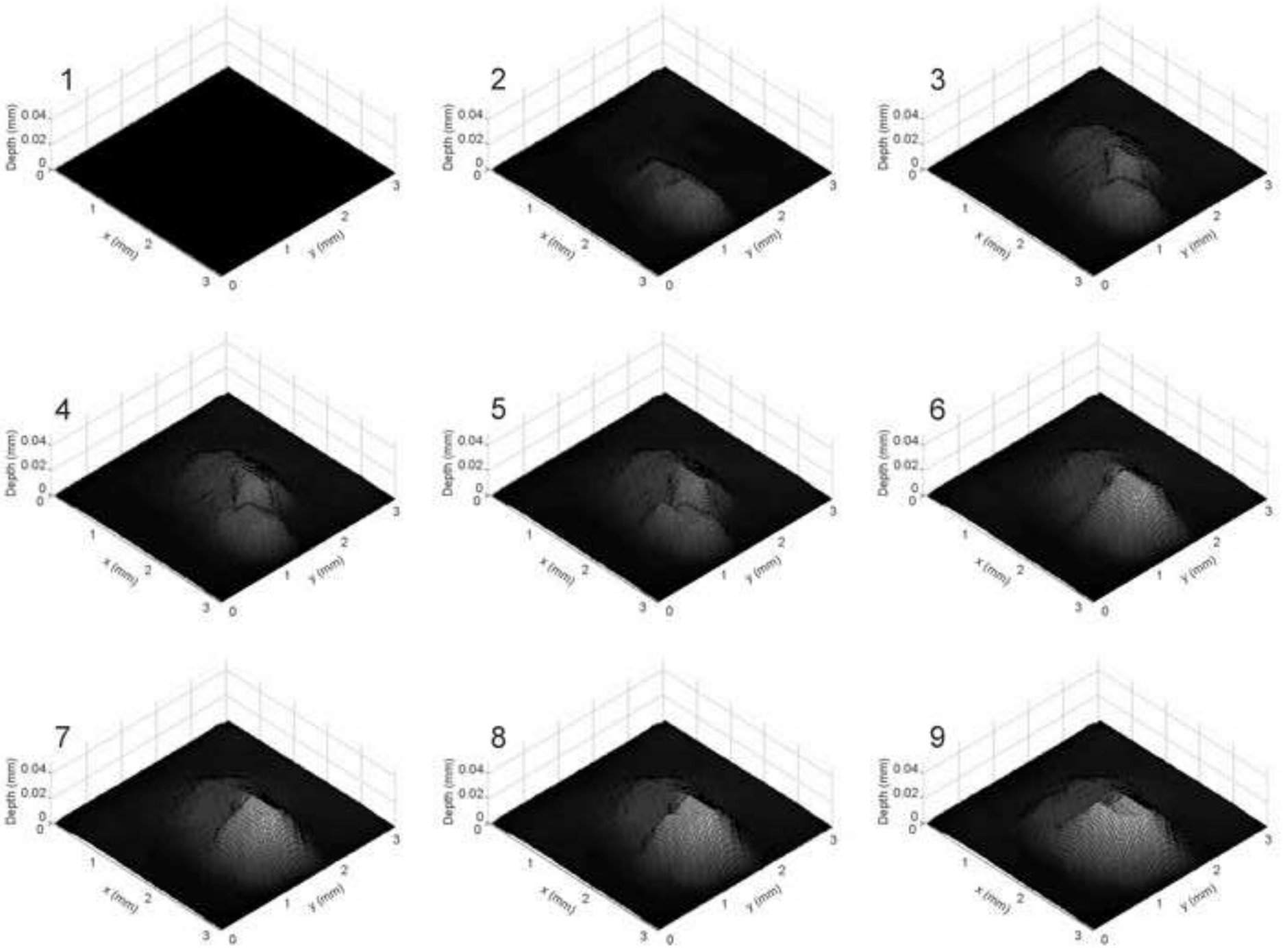

Figure11

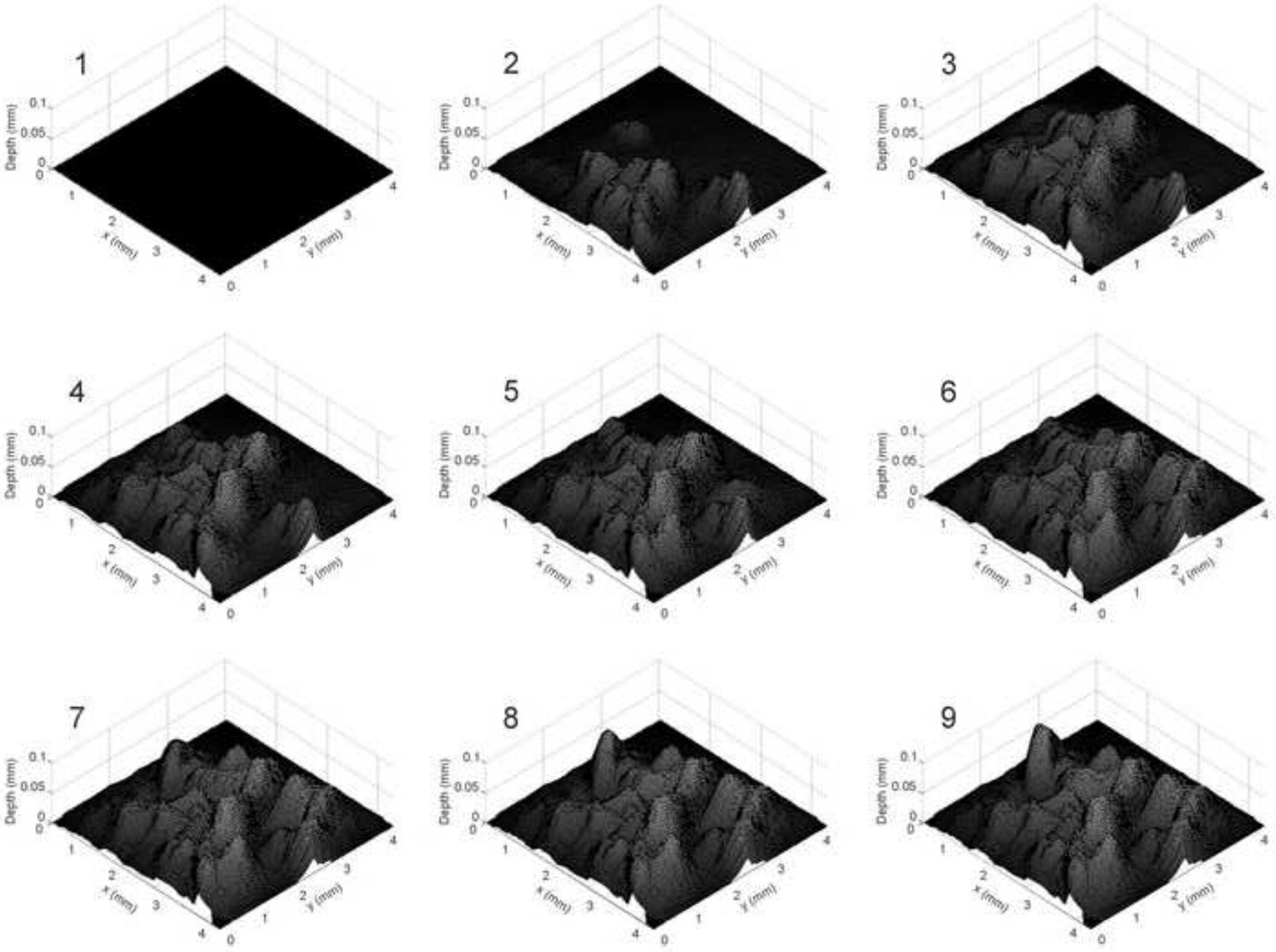

Figure12

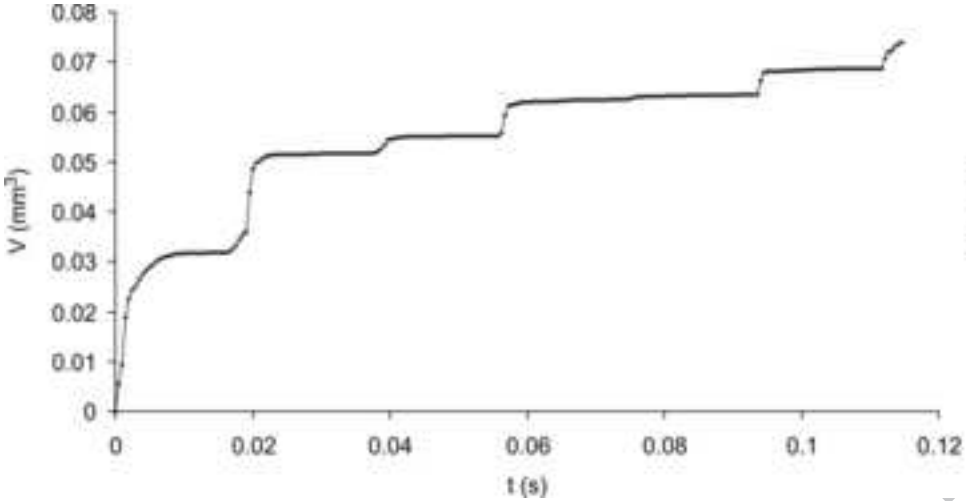

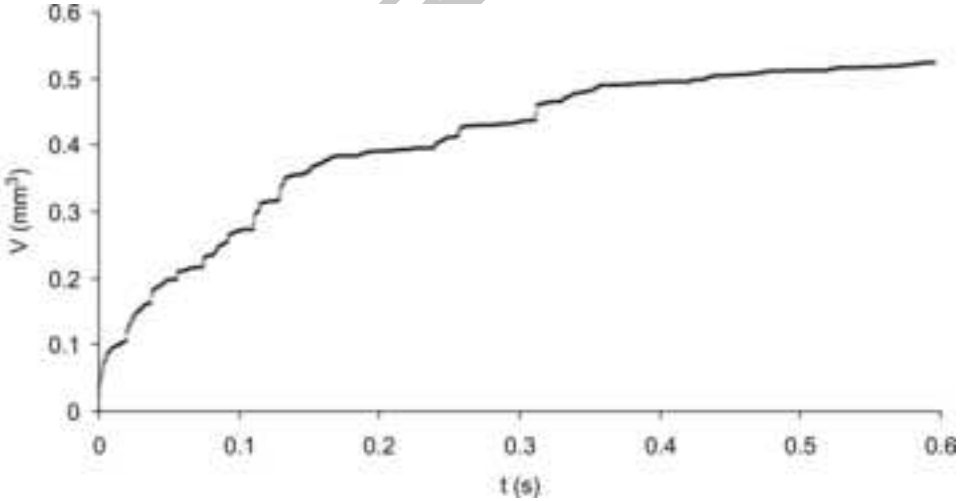

RESEARCH HIGHLIGHTS

Manuscript title:
Observation of cavitation erosion pit formation

Authors:
Matevž Dular (corresponding author)
Laboratory for Water and Turbine Machines, University of Ljubljana
Askerceva 6, 1000 Ljubljana, Slovenia
matevz.dular@fs.uni-lj.si
Tel: +386 1 4771 453
Fax: +386 1 2518 567

Olivier Coutier Delgosha
Laboratoire de Mécanique de Lille, ParisTech
8 Boulevard Louis XIV, 59046 Lille, France
olivier.coutier@ensam.eu

Martin Petkovšek
Laboratory for Water and Turbine Machines, University of Ljubljana
Askerceva 6, 1000 Ljubljana, Slovenia
martin.petkovsek@fs.uni-lj.si

Research highlights

- We used a novel approach (shape from shading) for high speed cavitation damage evaluation.
- It was found that large pits are actually pit clusters where individual pits overlap.
- We observed that thin foil behaves like a membrane which is also stretched when stress is applied.
- Resistance of the material against ultrasonic and hydrodynamic cavitation cannot be compared.

Yours sincerely,

Dr. Ing. Matevž Dular (corresponding author) Ljubljana, 2.4.2012